

## Supplementary Information

### **In-situ polymerization confining synthesis of ultrasmall MoTe<sub>2</sub> nanoparticles for electrochemical detection of dopamine**

Yuting Du, Linxiu Dai\*, Fan Yang, Yue Zhang, Changhua An\*

Tianjin Key Laboratory of Organic Solar Cell and Photochemical Conversion, School of Chemistry and Chemical Engineering, Life and Health Intelligent Research Institute, Tianjin University of Technology, Tianjin 300384, China

Email: linxiudai@163.com; anchua@ustc.edu

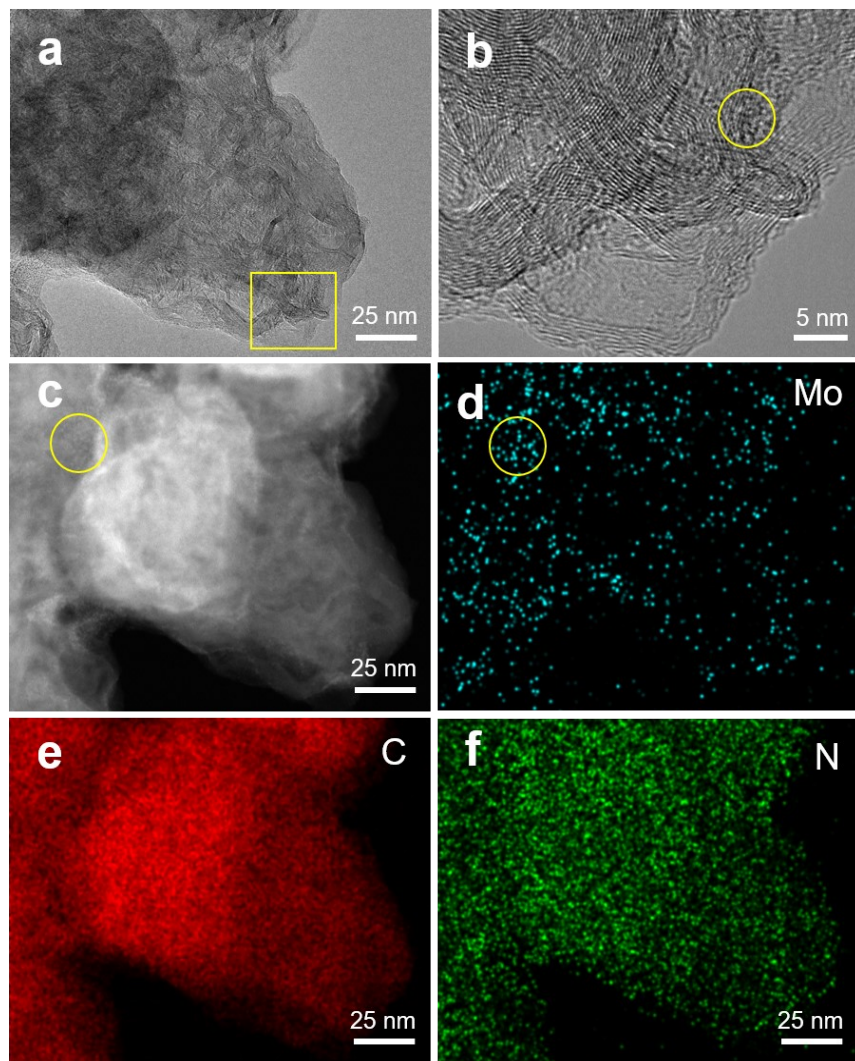


**Fig. S1.** Structural characterization of the as-obtained Mo@PPy/C. (a-b) TEM and HRTEM images (the inset shows the SAED pattern); (c-f) Element mapping images.

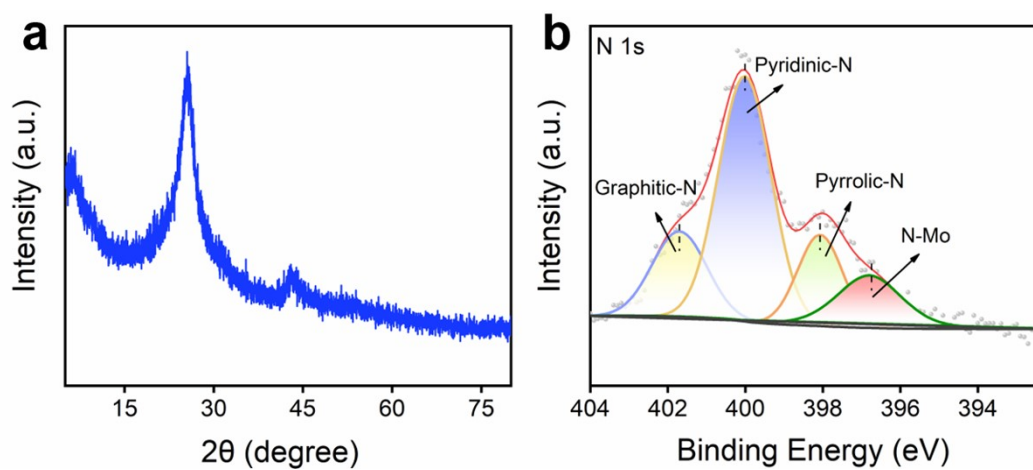


**Fig. S2.** (a) XRD pattern of Mo/PPy/C; (b) High-resolution XPS spectra of N elements in Mo/PPy/C.

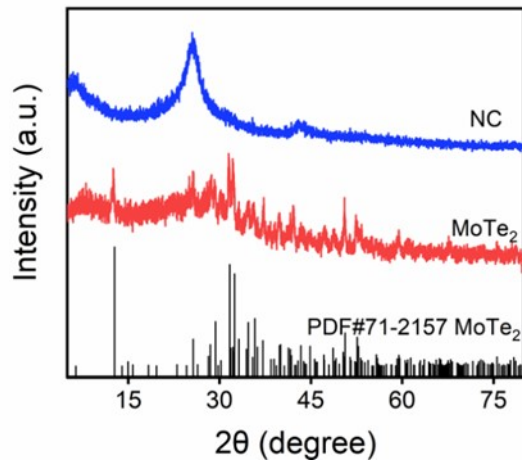


**Fig. S3.** XRD pattern of NC and bulk MoTe<sub>2</sub>.

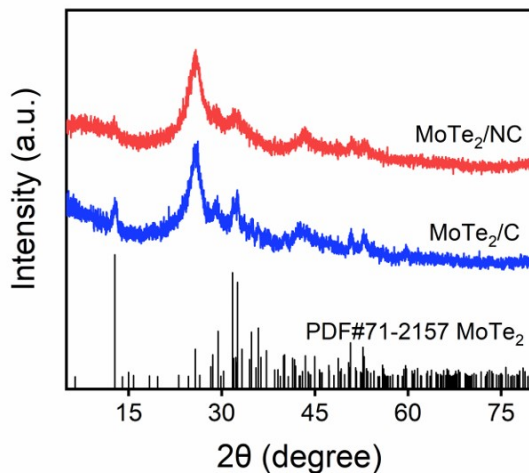


**Fig. S4.** XRD patterns of MoTe<sub>2</sub>/NC and MoTe<sub>2</sub>/C.

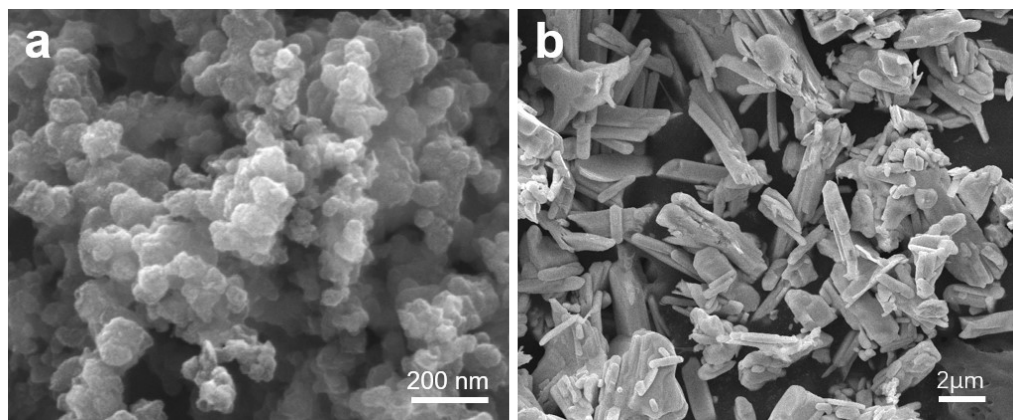


**Fig. S5.** High and low-magnification (inset) SEM images (a) NC and (b) bulk MoTe<sub>2</sub>.

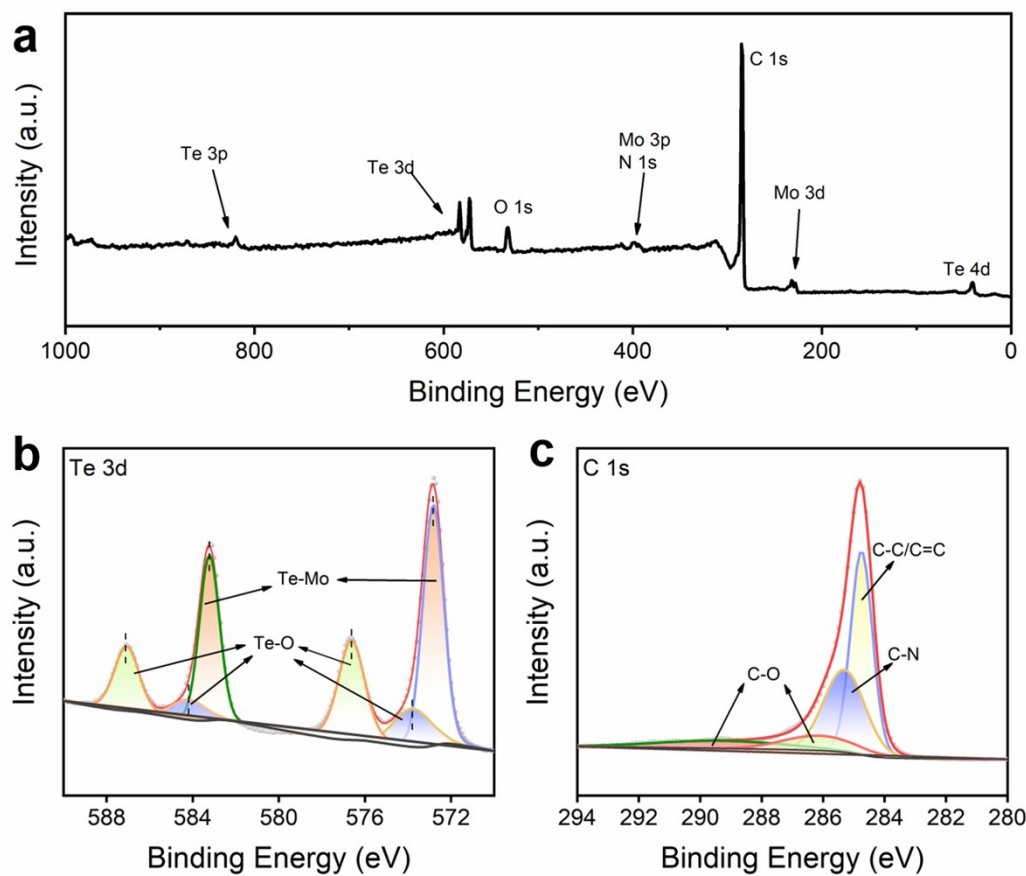


**Fig. S6.** High-resolution XPS of the total and respective elements in MoTe<sub>2</sub>/NC. (a) Survey spectrum; (b) Te 3d; (c) C 1s.

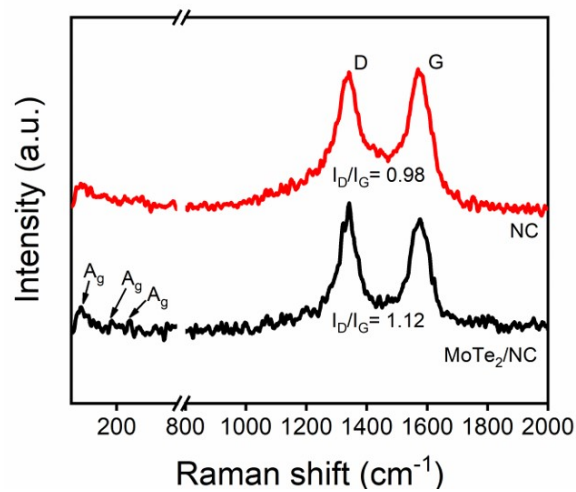


**Fig. S7.** Raman spectra of MoTe<sub>2</sub>/NC and NC.

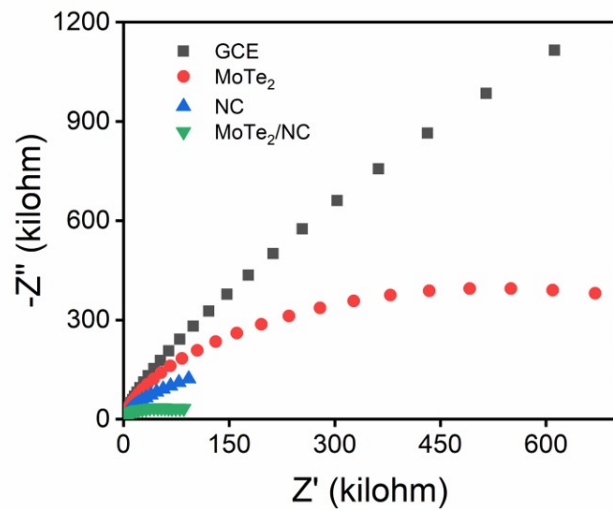


**Fig. S8.** EIS of different modified electrodes.

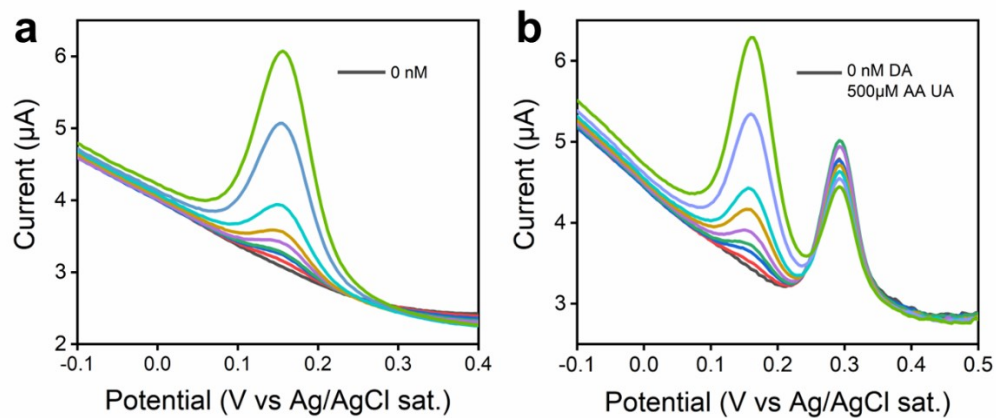


**Fig. S9.** (a) An enlarged image of Fig. 4a; (b) An enlarged image of Fig. 5b.

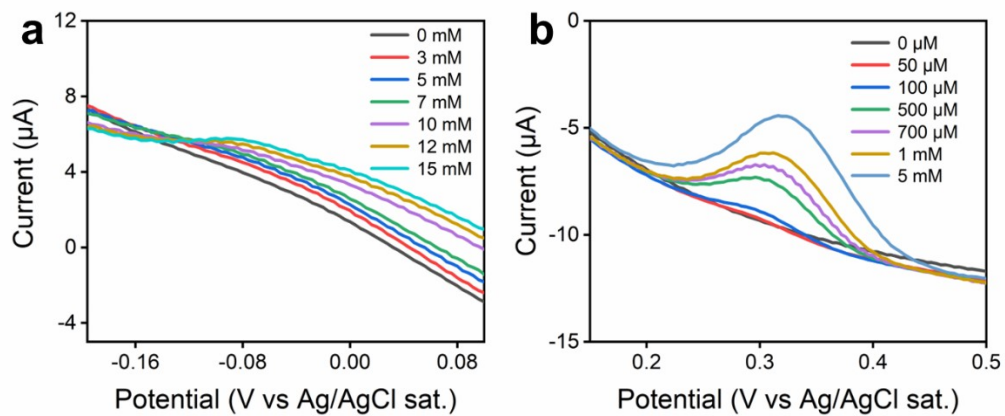


**Fig. S10.** DPV curves over MoTe<sub>2</sub>/NC for the detection of AA (a) and UA (b) under different concentrations.

**Table S1.** Performance comparisons with reported materials for detection of DA.

Materials	Linear detection range ( $\mu\text{M}$ )	LOD ( $\mu\text{M}$ )	References
MoS <sub>2</sub> NSs/N-Gr/GCE	3.2-5680	11.9	1
rGO-Co <sub>3</sub> O <sub>4</sub> /GCE	0-30	0.277	2
RGO-ZnO/GCE	1-70	0.33	3
Graphene/Pt-modified GCE	0.03-8.13	0.03	4
S-MoSe <sub>2</sub> /NSG/Au/MIPs	0.05-1110	0.02	5
Ag-Pt/pCNFs	100-500	0.11	6
Boron-CNT/GCE <sup>d</sup>	0.02-75	0.0014	7
Pt/MWCCNT/GCE	0.061-7.03	0.028	8
Nafion/Te NWs/GCE	0.005-1.0	0.001	9
MoTe <sub>2</sub> /NC/GCE	0.1-50	0.007	This work

## References

1. L. G. Bach, D. M. Nguyen, Q. B. Bui, P. H. Ai-Le and H. T. Nhac-Vu, *Mater. Chem. Phys.*, 2019, **236**, 121814.
2. A. Numan, M. M. Shahid, F. S. Omar, K. Ramesh and S. Ramesh, *Sens. Actuators, B*, 2017, **238**, 1043-1051.
3. X. Zhang, Y. Zhang and L. Ma, *Sens. Actuators, B*, 2016, **227**, 488-496.
4. C.-L. Sun, H.-H. Lee, J.-M. Yang and C.-C. Wu, *Biosens. Bioelectron.*, 2011, **26**, 3450-3455.
5. Y. Zang, J. Nie, B. He, W. Yin, J. Zheng, C. Hou, D. Huo, M. Yang, F. Liu, Q. Sun, Y. Qin and H. Fa, *Microchem. J.*, 2020, **156**, 104845.
6. Y. Huang, Y.-E. Miao, S. Ji, W. W. Tjiu and T. Liu, *ACS Appl. Mater. Interfaces*, 2014, **6**, 12449-12456.
7. C. Deng, J. Chen, M. Wang, C. Xiao, Z. Nie and S. Yao, *Biosens. Bioelectron.*, 2009, **24**, 2091-2094.
8. Z. Dursun and B. Gelmez, *Electroanalysis*, 2010, **22**, 1106-1114.
9. H. Tsai, Z. Lin and H. Chang, *Biosens. Bioelectron.*, 2012, **35**, 479-483.